Journal of Experimental Botany, Vol. 62, No. 6, pp. 2205–2215, 2011
doi:10.1093/jxb/erq428 Advance Access publication 13 January, 2011
This paper is available online free of all access charges (see http://jxb.oxfordjournals.org/open_access.html for further details)

Journal of Experimental Botany
www.jxb.oxfordjournals.org

RESEARCH PAPER

The rate of nitrite reduction in leaves as indicated by O_2 and CO_2 exchange during photosynthesis

H. Eichelmann[1], V. Oja[1], R.B. Peterson[2] and A. Laisk[1,*]

[1] Institute of Molecular and Cell Biology, Tartu University, Riia st. 23, Tartu 51010, Estonia

[2] Department of Biochemistry and Genetics, The Connecticut Agricultural Experiment Station, 123 Huntington St., New Haven, CT 06511, USA

* To whom correspondence should be addressed: E-mail: alaisk@ut.ee

Received 17 June 2010; Revised 25 November 2010; Accepted 26 November 2010

Abstract

Light response (at 300 ppm CO_2 and 10–50 ppm O_2 in N_2) and CO_2 response curves [at absorbed photon fluence rate (PAD) of 550 μmol m^{-2} s^{-1}] of O_2 evolution and CO_2 uptake were measured in tobacco (*Nicotiana tabacum* L.) leaves grown on either NO_3^- or NH_4^+ as N source and in potato (*Solanum tuberosum* L.), sorghum (*Sorghum bicolor* L. Moench), and amaranth (*Amaranthus cruentus* L.) leaves grown on NH_4NO_3. Photosynthetic O_2 evolution in excess of CO_2 uptake was measured with a stabilized zirconia O_2 electrode and an infrared CO_2 analyser, respectively, and the difference assumed to represent the rate of electron flow to acceptors alternative to CO_2, mainly NO_2^-, SO_4^{2-}, and oxaloacetate. In NO_3^--grown tobacco, as well as in sorghum, amaranth, and young potato, the photosynthetic O_2–CO_2 flux difference rapidly increased to about 1 μmol m^{-2} s^{-1} at very low PADs and the process was saturated at 50 μmol quanta m^{-2} s^{-1}. At higher PADs the O_2–CO_2 flux difference continued to increase proportionally with the photosynthetic rate to a maximum of about 2 μmol m^{-2} s^{-1}. In NH_4^+-grown tobacco, as well as in potato during tuber filling, the low-PAD component of surplus O_2 evolution was virtually absent. The low-PAD phase was ascribed to photoreduction of NO_2^- which successfully competes with CO_2 reduction and saturates at a rate of about 1 μmol O_2 m^{-2} s^{-1} (9% of the maximum O_2 evolution rate). The high-PAD component of about 1 μmol O_2 m^{-2} s^{-1}, superimposed on NO_2^- reduction, may represent oxaloacetate reduction. The roles of NO_2^-, oxaloacetate, and O_2 reduction in the regulation of ATP/NADPH balance are discussed.

Key words: CO_2 uptake, nitrite reduction, O_2 evolution, photosynthesis.

Introduction

The metabolic pathway of N assimilation is well established in leaves (Foyer and Noctor, 2002). In the cytosol, nitrate (NO_3^-) is reduced to nitrite (NO_2^-) by nitrate reductase (NR) at the expense of NADH produced from malate shuttled from the mitochondrion or chloroplast. Nitrite enters the chloroplast either as the neutral acid HNO_2 or with the help of a transporter (Brunswick and Cresswell, 1988*a*; *b*; Shingles *et al.*, 1996). Photosynthetically generated reduced ferredoxin (Fd^-) is used for the reduction of one NO_2^- to NH_4^+ and 1.5 O_2 are evolved (Swader and Stocking, 1971). Ammonia is combined with 2-oxoglutarate (OG) via the glutamine–glutamate cycle (GS/GOGAT) to form glutamate (Anderson and Done, 1978). In leaves, the reductive steps of this pathway consume Fd^- at the expense of photosynthetic CO_2 fixation. This offers the possibility for *in vivo* measurement of NO_2^- reduction as the surplus of O_2 evolution over CO_2 fixation.

Abbreviations: A_C, A_O, CO_2 and O_2 exchange rates; AQ, assimilatory quotient; CET, cyclic electron transport; Fd, ferredoxin; F_m, F, F_0, fluorescence yield - pulse-saturated, steady-state, and minimum under FRL, respectively; FRL, far-red light; FNR, ferredoxin-NADP reductase; Gln, glutamine; Glu, glutamate; GS/GOGAT, glutamine synthase/glutamate synthase; NR, nitrate reductase; NiR, nitrite reductase; NPQ, non-photochemical quenching; OG, 2-oxoglutarate; OA, oxaloacetate; PAD, PFD, photon fluence rate, absorbed and incident; PEP, phosphoenolpyruvate; PGA, 3-phosphoglyceric acid; PSII, PSI, photosystems II and I; qE, rapid, H^+-dependent phase of NPQ; R_L, R_D, respiration rates in the light and in the dark; Φ_C, Φ_O, quantum yield of electron transport calculated from A_C and A_O.

© 2011 The Author(s).

This is an Open Access article distributed under the terms of the Creative Commons Attribution Non-Commercial License (http://creativecommons.org/licenses/by-nc/2.5), which permits unrestricted non-commercial use, distribution, and reproduction in any medium, provided the original work is properly cited.

Recent reports from this laboratory suggest that cyclic electron transport (CET) around PSI is uncoupled from H^+ translocation, and hence does not support photophosphorylation (Laisk *et al.*, 2007, 2008, 2010). This shifts attention to NO_2^- reduction as a means to compensate for imbalances in the production/utilization ratios of ATP and NADPH. During linear electron transport from H_2O to NADP, 4 e^- (2 NADPH) co-transport 12 H^+ that, in turn, support the synthesis of 3 ATP. This is just sufficient to drive the assimilation of one CO_2 through the Calvin–Benson cycle (Laisk *et al.*, 2007). However, any extra ATP needed for chloroplast secondary metabolism, for example, starch and protein synthesis, must be generated at the expense of electron transport to acceptors other than CO_2 and involve metabolic pathways that do not consume as much ATP per e^- as CO_2 reduction does. Considering that the Mehler reaction and SO_4^{2-} reduction (on average, 19% of NO_2^- reduction, Hirasawa *et al.*, 2004; Kopriva, 2006) plus a presumably much slower rate of reduction of enzyme disulphide groups must accompany photosynthesis, it has been a challenge to establish whether a specific link exists between NO_2^- reduction and the production of extra ATP for CO_2 reduction (Noctor and Foyer, 1998). Mathematical modelling of N and C metabolism suggested that N limitation, common in natural communities, may proportionally limit CO_2 assimilation and help maintain a rather constant N/C ratio in plants (Laisk *et al.*, 2009).

Although the pathway is biochemically well established, how NO_2^- reduction is regulated and its relationship to photosynthesis are largely unknown. In isolated intact plastid preparations, NO_2^- photoreduction displayed rates of 8–22 μmol h^{-1} mg^{-1} Chl, while rates of CO_2 fixation varied from zero to 90 μmol h^{-1} mg^{-1} Chl depending on the bicarbonate concentration employed (Robinson, 1986). Considering that in these experiments photoassimilation of each NO_2^- required 8 e^- (6 e^- to reduce NO_2^- to NH_4^+ plus 2 e^- to assimilate NH_4^+ into Glu) but CO_2 assimilation required only 4 e^- per molecule, electron flow rate was divided roughly equally between C and N reduction under these experimental conditions, but CO_2 reduction dominated at higher CO_2 concentrations. The results suggested that, if substrates are available, then the enzymic capacity of NO_2^- photoreduction may be comparable to that of CO_2 reduction. More importantly, under saturating CO_2 supply the rate of CO_2 fixation was stimulated when simultaneous NO_2^- photoreduction was supported, as expected if NO_2^- reduction facilitates balancing of ATP and NADPH. However, these *in vitro* rates may differ from actual *in vivo* rates because of different substrate availabilities.

In vivo information about NO_2^- and CO_2 reduction can be derived from simultaneous measurements of O_2 evolution and CO_2 uptake during photosynthesis. When carbohydrate is the sole product then the assimilatory quotient ($AQ=CO_2/O_2$ flux ratio) is 1.0. Any decrease in this quotient below 1.0 (surplus of O_2 evolution) would indicate electron flow to acceptors other than CO_2 (Cen *et al.*, 2001). Early manometric measurements of CO_2/O_2 exchange during photosynthesis were reported by Warburg (1948). Today the most sophisticated methods are based on mass spectrometry, which allows one to measure the uptake and evolution components of CO_2 and O_2 fluxes (Badger *et al.*, 2000; Ruuska *et al.*, 2000; Siebke *et al.*, 2003). Such measurements showed that less than 10% of the photosynthetic electron flow is diverted to alternative acceptors in C_3 plants, but more in C_4 plants. Stabilized zirconia O_2 analysers were first applied to the measurement of O_2 evolution from intact leaves by Björkman and Gauhl (1970). For reliable measurement of the O_2/CO_2 exchange ratio at the atmospheric O_2 level (210 000 ppm), concentrations and flow rates must be held constant to within a factor of at least 10^{-5}. This difficult technical problem was solved by Bloom *et al.* (1989) who reported that, in barley shoots at high light intensities, O_2 evolution was in excess of CO_2 uptake by as much as 26% when plants were fed NO_3^-, but there was no excess O_2 evolution when the plants were fed NH_4^+. Nitrogen reduction (excess O_2 evolution) increased with light intensity, causing a decrease in AQ of 10–15% (Bloom *et al.*, 2002; Rachmilevitch *et al.*, 2004). These simultaneous measurements of O_2 evolution and CO_2 uptake resulted in reliable values of daily integral CO_2 and O_2 exchange, but the environmental dependencies of nitrite reduction rate and its relationship to photosynthesis were not studied.

Using an experimental approach developed in the Tartu laboratory, O_2/CO_2 measurements were carried out in an atmosphere containing a very low O_2 concentration of 10–50 ppm. Although anaerobiosis can be lethal when imposed over an extended time, it is free of negative after-effects when applied for shorter intervals (up to about 30 min). The expedient of blocking all O_2 uptake processes significantly increases the precision of O_2 evolution measurements and simplifies data interpretation. Hence, the principal development is supported as methodological capabilities expand. Our measurements revealed highly proportional responses between O_2 evolution and CO_2 uptake rates ($r^2=0.9999$) with the slope varying from 0.99 to 1.01 in potato leaves (Laisk *et al.*, 2007). Unexpectedly, these measurements indicated the complete absence of significant surplus O_2 evolution supporting NO_2^- or OA reduction. Since NO_2^- reduction was, nevertheless, expected to be present, it is suggested that carbon skeletons for amino acid synthesis are partitioned from the photosynthetic PGA pool before its reduction. Thus, the O_2/CO_2 ratio would be <1 for carbon metabolism but would rise to unity after the extra O_2 evolved during NO_2^- reduction is added. A corresponding mathematical model, considering also some PEP carboxylation, satisfactorily reproduced the measured O_2/CO_2 ratio (Laisk *et al.*, 2009).

Our previous work (Laisk *et al.*, 2007) explored the relationships between O_2 and CO_2 fluxes over the entire light and CO_2 response ranges of photosynthesis, so that data points measured at high gas exchange rates carried greater weight than those measured near the light and CO_2 compensation points. Important also in these measurements, the respiratory CO_2 evolution rate was assumed to be constant over the light response curve. Contrary to this,

significant changes in respiratory O_2/CO_2 fluxes have been shown to be related to NO_3^- assimilation (Cousins and Bloom, 2004). In the present work, the O_2 and CO_2 exchange measurements were repeated, focusing on differences at low light intensities and considering light-induced changes in the respiratory rate. Instead of the CO_2/O_2 ratio (assimilatory quotient), the absolute rate of surplus (excess) photosynthetic O_2 evolution relative to photosynthetic CO_2 uptake is presented, which is a measure of the total rate of alternative electron transport (Cen *et al.*, 2001). By comparing tobacco plants grown with NO_3^- or NH_4^+ as the N source it is shown that NO_2^- reduction and CO_2 reduction compete for one and the same pool of reductant with similar affinity. At low light intensities (<50 μmol quanta m^{-2} s^{-1}) NO_2^- reduction saturates at a rate corresponding to about 1 μmol O_2 m^{-2} s^{-1}, while CO_2 reduction continues to increase with light [since measured under relatively reductive conditions (absence of O_2) the reported N reduction rate may be even somewhat overestimated]. At high light intensities, another process of surplus O_2 evolution increases to about 1 μmol O_2 m^{-2} s^{-1}, which is suggested to be the reduction of OA.

Materials and methods

Plants and growth conditions

Plants were grown in a growth chamber (AR-95HIL, Percival, from CLF Plant Climatics GmbH, Emersacker, Germany) at a PFD of 470–670 μmol quanta m^{-2} s^{-1}, 14/10 h day/night cycle, 25/20 °C temperature, and relative humidity of 60–65%. Seeds of tobacco (*Nicotiana tabacum* L.) were germinated and plants were grown in a 250 cm^3 block of rock wool partially submerged in nutrient solution. The nutrient solution was based on the Knop formula in two versions, containing either 4 mM $Ca(NO_3)_2$ or 4 mM $(NH_4)_2SO_4$ as the N source. The blocks were washed and the nutrient solution was changed weekly. Attached leaves of 8–10-week-old plants (about 80% of full leaf expansion) were used in experiments. The C_4 plants *Sorghum bicolor* L. Moench and *Amaranthus edulis* L. were grown in 8.0 l pots on peat and watered with NH_4NO_3 Knop solution weekly.

Potato plants (*Solanum tuberosum* L.) were grown in the laboratory at a PFD of 400–600 μmol quanta m^{-2} s^{-1} and a 14/10 h day/night regime and temperature of 22–25/16–18 °C. A second set of plants was grown in the field as described by Laisk *et al.* (2007). Fully expanded attached leaves of laboratory-grown plants were used in the experiments. Mature leaves from field-grown plants were cut early in the morning and kept in the dark with petioles immersed in water until measurements commenced.

Seed of the zeaxanthin epoxidase-defective *aba 1-6* mutant of *Arabidopsis thaliana* (Col-0) was obtained from the Arabidopsis Biological Resource Centre (stock CS3772). Plants were grown at 130 μmol quanta m^{-2} s^{-1} under a 23/20 °C, 16/8 h day/night regime.

Gas exchange measurement system

A two-channel leaf gas exchange measurement system (Laisk and Oja, 1998; Fast-Est Instruments, Tartu, Estonia) enabled the control of CO_2, H_2O, and O_2 pressures and measurement of CO_2, H_2O, and O_2 exchange (for performance see Laisk *et al.*, 2002; Oja *et al.*, 2003). The leaf was enclosed in a 32 mm diameter by 3 mm deep chamber and flushed with gas at a flow rate of 0.5 mmol s^{-1}. To stabilize leaf temperature and fix the leaf for optical measurements, the upper epidermis was sealed with starch paste to a glass window in contact with a water jacket. Gas exchange occurred through the lower epidermis. The water jacket temperature was 22 °C and leaf temperature was maintained at 22±0.3 °C over the range of actinic light intensities used.

The leaf chamber was illuminated by three sources through a multi-branched fibre-optic light guide. Plastic fibres (1 mm, Toray Polymer Optical Fiber, PF series, from Laser Components, Gröbenzell/München, Germany) were individually arranged to produce uniform illumination of the chamber-enclosed adaxial leaf surface for each source (Laisk and Oja, 1998; Oja *et al.*, 2010). Actinic white light and saturation pulses (10 000 μmol quanta m^{-2} s^{-1}, 1–3 s length) were provided by separate tungsten-halogen KL 1500 sources (H Walz, Effeltrich, Germany) each equipped with a far-red blocking filter and an electro-pneumatic shutter with flying time of 1.3 ms (Fast-Est Instruments, Tartu, Estonia). Far red illumination (50 μmol quanta m^{-2} s^{-1} at 720 nm) was provided by a laboratory-built light-emitting diode array (Laisk *et al.*, 2010).

Simultaneous CO_2 and O_2 exchange measurements

Rates of CO_2 exchange were measured with an infrared gas analyser LI- 6251 (Li-Cor, Lincoln, NE, USA). Evolution of O_2 was measured in the same gas flow with a calcia zirconia O_2 analyser (S-3A, Ametek, Pittsburgh, PA, USA) on a minimum background of 10 ppm O_2 in N_2 (during active photosynthesis the O_2 concentration at the chamber outlet increased to 40–50 ppm). Since differences between CO_2 and O_2 fluxes were small, both gas analysers were precisely calibrated based on a method developed for simultaneous O_2/CO_2 measurements (Oja *et al.*, 2007). The method calibrates the CO_2 and O_2 scales on the basis of O_2 concentration measurements. Pure CO_2 and O_2 were separately forced to flow through one and the same capillary at the same pressure difference and into a known flow of CO_2-free dry air containing 20.94% O_2. The relative increase in O_2 concentration due to the addition of pure O_2 and the decrease in O_2 concentration due to the addition of pure CO_2 were measured with the O_2 analyser. The CO_2 and O_2 flow rates through the capillary were calculated creating a complete calibration function for CO_2 and O_2 over the full range of pressures applied to the capillary with a relative standard deviation of <1%. These flow rate data could then be used for the routine calibration of O_2 and CO_2 analysers. The accuracy of the method rests solely on the well-known concentration of O_2 in the atmosphere. The CO_2 scales coincided exactly with a factory calibration of a LI-7000 CO_2 analyser, attesting to the correctness of the calibration procedure. The response time of the O_2 analyser was 0.8 s and that of the CO_2 analyser was 1.6 s.

Accompanying measurements

Cell wall and chloroplast CO_2 concentrations were routinely calculated. Mesophyll diffusion resistance was determined from simultaneous CO_2 exchange and Chl fluorescence measurements (Laisk *et al.*, 2002). Chl fluorescence was measured with a PAM-101 and ED-101 emitter-detector (H. Walz, Effeltrich, Germany). Values of PSII quantum efficiency were calculated from Chl fluorescence parameters as $(F_m–F)/F_m$ where F was measured in the presence of actinic light and F_m was measured during a superimposing saturation pulse. Rubisco content and k_{cat} (s^{-1}) were measured as described earlier (Laisk *et al.*, 2002; Eichelmann *et al.*, 2009). Electron transport rate for PGA reduction in the presence of photorespiration was calculated considering the Rubisco CO_2/O_2 specificity factor and chloroplast dissolved CO_2 and O_2 concentrations (Laisk *et al.*, 2002). The content of organic N in leaves was measured by the micro-Kjeldahl method (Kjeltech Auto 1030, Foss Tecator AB, Hoeganaes, Sweden). Experimental procedures were pre-programmed into a text file and data were recorded using an A/D converter (ADIO 1600, Kontron, San Diego, CA) and a system-operation and data-recording program RECO (Fast-Est Instruments, Tartu, Estonia).

Results

Effects of different N nutrition on plant growth

Plants grew faster on NO_3^- than on NH_4^+ (Fig. 1). Nevertheless, photosynthetic rates per unit leaf area were faster in the NH_4^+-grown compared to the NO_3^--grown plants (Table 1). There was no indication of ammonia-induced electron-proton uncoupling in photosynthesis. In contrast to photosynthetic rate, area-based total organic N, and Chl contents were higher in NO_3^--grown plants than in NH_4^+-grown plants. Higher gas phase (stomatal) resistance and lower Rubisco k_{cat} together significantly limited photosynthesis in NO_3^--grown plants. After an NH_4^+-grown plant was transferred to NO_3^-, the emerging new leaves showed much faster photosynthetic rates due to lower gas phase resistance and higher Rubisco k_{cat}. Thus, NO_3^--grown and NH_4^+-grown plants grew under different types of stress. The stress associated with growth on NH_4^+ was eased after transfer to NO_3^- nutrition.

Light response of O_2 evolution and CO_2 uptake in C_3 plants

Figure 2 shows the pre-programmed sequence of procedures employed during measurement of a light response curve. The initial light intensity was 538 μmol absorbed quanta m^{-2} s^{-1} (PAD). Subsequently, the PAD was increased to 930 μmol m^{-2} s^{-1} and then decreased stepwise to zero. The exposure lasted 80 s at each PAD, sufficient to establish a steady-state. Next, a saturation pulse was applied to measure F_m, after which the actinic light was turned off for 10 s to record the O_2 analyser baseline (FRL was added during the darkening for 2 s prior to measuring F_0).

The saturation pulse induced a sharp peak of O_2 evolution, followed by a return to the baseline during the 10 s of darkness. The temporal response of CO_2 uptake to a change in PAD lagged that of O_2 evolution, but not because of instrumental response. Upon darkening, the CO_2 uptake rate declined slowly, because the RuBP pool (and some ATP, proton gradient, and NADPH, see Kirschbaum and Pearcy, 1988) supported post-illumination CO_2 fixation. When light was restored, these pools slowly regenerated during induction of CO_2 uptake accompanied by fast O_2 evolution at non-limiting PADs. The entire measurement routine lasted 1000 s, during which time the leaf was under low O_2. This, however, did not cause any irreversible change in the photosynthetic response; neither did the leaf appear injured during subsequent growth.

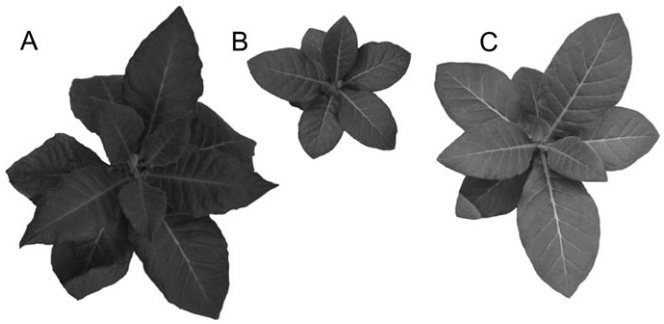

Fig. 1. Nine-week-old tobacco plants grown on NO_3^- (A) and NH_4^+ (B), and the same NH_4^+-grown plant 2 weeks after transfer to NO_3^- (C).

Analysis of O_2 and CO_2 exchange rates is complicated by different dark rates of these processes. The rate of O_2 uptake was assumed to be zero in the dark, since the residual O_2 concentration was only about 10 ppm in the N_2 used and the K_m (O_2) of the respiratory cytochrome *c* oxidase is 185 ppm (Laisk et al., 2007). By contrast, CO_2 evolution from all respiratory decarboxylations continued during the anaerobiosis without significant change. Therefore, the O_2 evolution signal reflected photosynthesis only, while the CO_2 uptake signal reflected the sum of photosynthetic carboxylation and respiratory decarboxylation processes. In an earlier report (Laisk *et al.*, 2007), O_2 and CO_2 exchange was compared directly by plotting the O_2 rate against the CO_2 rate. Such a plot for the experiment of Fig. 2 is shown in Fig. 3. For rates exceeding 3 μmol m^{-2} s^{-1} the regression is highly linear with slope 1.006 (r^2=0.9999). At lower rates (low PADs) data points depart from the regression line. In this work, the focus is on these latter small deviations whose rates are comparable to the rate of respiratory CO_2 evolution in the light.

CO_2 response of O_2/CO_2 exchange and light response of respiration

Respiratory CO_2 evolution in the light was measured using the *A* versus C_c response of leaf gas exchange at a PAD of 531 μmol quanta m^{-2} s^{-1} (Fig. 4). Extrapolated to C_c=0, the CO_2 uptake rate was –0.68 μmol m^{-2} s^{-1} in the light. The rate of O_2 evolution remained faster than that of CO_2 uptake by a constant difference of 2.66 μmol m^{-2} s^{-1} at all C_c values, including zero. At this saturating PAD this A/C_c response shows the maximum degree of suppression of respiratory CO_2 evolution in the light, i.e. from –1.27 in the dark to –0.68 μmol m^{-2} s^{-1} in the light. In further analysis, it is assumed that the rate of respiratory CO_2 evolution decreased from the dark value to that measured in saturating light along a smooth curve (equation 1) in parallel with the photosynthetic O_2 evolution rate:

$$R_L = R_D[1 - C(A_{PAD}/A_{max})^{\alpha}] \quad (1)$$

where A_{PAD} is the O_2 evolution rate at a given PAD, A_{max} is the maximum, α=0.5, and *C* is the fractional maximum suppression of dark respiration.

Light dependence of surplus O_2 evolution

Figure 5 shows an analysis which considers the light response of dark (mitochondrial) respiration. The measured difference A_O–A_C equals the respiratory CO_2 evolution rate in the dark (since O_2 evolution=0 in the dark under our experimental conditions), but this difference rapidly increases to 2.75 μmol m^{-2} s^{-1} at a PAD of 50 μmol quanta m^{-2} s^{-1}. Then, A_O–A_C passes through a small trough over

Table 1. General properties of leaves

FW, fresh weight; DW, dry weight; N, total organic N content; Rubisco, Rubisco content; Chl, chlorophyll; A_C(13μM), CO_2 uptake rate at ambient dissolved CO_2 concentration, C_{w0}, of 13 μM (360 ppm), 21% O_2 (air); A_C(50μM), CO_2 uptake rate at C_{w0} of 50 μM, 21% O_2 (CO_2 saturation); R_D, dark respiration; r_{gw}, gas phase resistance in air; k_{cat}, Rubisco maximum turnover rate; Φ_O, maximum quantum yield of electron transport calculated from O_2 evolution; Φ_N maximum quantum yield of N reduction; A_O(11μM), light-saturated O_2 evolution rate at ambient dissolved CO_2 concentration of 11 μM (300 ppm), 10 ppm O_2; A_O/A_C, linear regression slope of O_2 evolution versus CO_2 uptake; ΔA_O(50μE), surplus O_2 evolution at PAD=50 μmol quanta m^{-2} s^{-1}; ΔA_O(1000μE), surplus O_2 evolution at PAD=1000; $\Delta A_O/A_O$ (50μE), surplus O_2 evolution ratio to O_2 evolution at PAD=50.

		Tobacco			C_4		Potatoes	
		NO_3^-	NH_4^+	NH_4^+ to NO_3^-	Sorghum	Amaranth	Laboratory	Field
FW	g m^{-2}	351±12	305±8	338±13	190±6	211±11	305±29	266±7
DW	g m^{-2}	64±5	73±4	41±4	26±3	31±1	40±6	39±1
N	g m^{-2}	2.9±0.1	1.9±0.3	1.9±0.1	1.4±0.1	2.1±0.1	3.0±0.4	2.1±0.1
Rubisco	g m^{-2}	3.3±0.4	2.8±0.8	2.9±0.1	1.3±0.1	2.2±0.1	5.1±0.5	4.0±0.2
Chl	μmol m^{-2}	666±33	318±126	327±43	411±11	384±47	580±22	438±14
A_C(13μM)	μmol m^{-2} s^{-1}	6.2±0.6	14.1±2.4	14.6±0.9	27.1±1.2	6.9±1.1	20.2±1.9	16.5±0.0
A_C(50μM)	μmol m^{-2} s^{-1}	20.6±2.3	32.3±7.9	35.4±0.6	34.0±1.6	12.6±1.7	41.8±4.9	37.6±1.3
R_D	μmol m^{-2} s^{-1}	–1.02±0.03	–1.60±0.48	–1.28±0.11	–0.75±0.11	–0.97±0.26	–1.24±0.16	–1.24±0.06
r_{gw}	s mm^{-1}	1.49±0.20	0.40±0.03	0.46±0.06	0.36±0.02	0.78±0.04	0.36±0.03	0.49±0.03
k_{cat}	s^{-1}	1.0±0.0	1.6±0.1	2.3±0.2	2.13±0.05	1.01±0.08	1.8±0.11	1.8±0.08
Φ_O	$e^-/h\nu$	0.218±0.008	0.295±0.007	0.349±0.015	0.246±0.005	0.255±0.020	0.332±0.009	0.313±0.004
Φ_N	$e^-/h\nu$	0.163±0.024	0.149±0.021	0.254±0.017	0.123±0.023	0.179±0.061	0.166±0.026	–
A_O(11μM)	μmol m^{-2} s^{-1}	7.1±0.6	16.1±1.1	19.1±2.4	24.6±2.0	12.5±0.6	22.8±2.2	22.4±1.1
A_O/A_C	regression	1.004±0.011	0.994±0.027	1.034±0.009	1.035±0.003	1.026±0.006	1.007±0.012	1.007±0.003
ΔA_O(50μE)	μmol m^{-2} s^{-1}	0.83±0.09	0.23±0.20	1.44±0.17	0.45±0.08	0.84±0.11	0.535±0.100	0.116±0.041
ΔA_O(1000μE)	μmol m^{-2} s^{-1}	0.87±0.09	0.55±0.32	1.82±0.30	1.48±0.29	1.12±0.16	0.964±0.197	0.778±0.091
$\Delta A_O/A_O$(50μE)		0.305±0.028	0.065±0.062	0.190±0.010	0.116±0.046	0.323±0.042	0.129±0.021	0.071±0.026

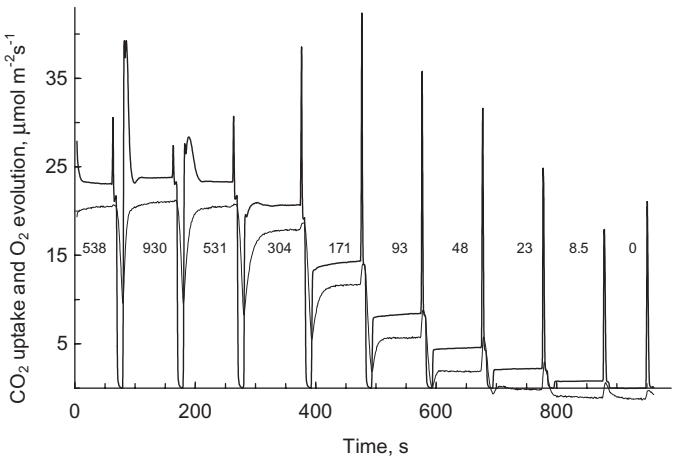

Fig. 2. Routine measurement sequence for the light response of O_2 evolution (thick line) and CO_2 uptake (thin line). The PAD (μmol quanta m^{-2} s^{-1}) was varied as indicated. At each PAD the stabilization time was 80 s, followed by a fluorescence saturation pulse, and then darkness for 10 s plus FRL for 2 s. Duration of the pulse was 1.4 s, except 2, 2.5, 3, and 3.5 s at PADs of 48, 23, 8.5, and 0 μmol quanta m^{-2} s^{-1}, respectively.

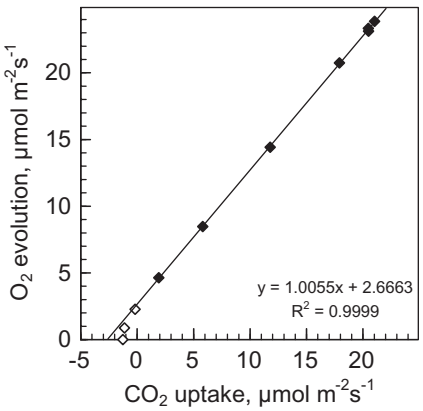

Fig. 3. Linear regression of O_2 evolution versus CO_2 uptake rates for the light response curve of Fig. 2 (only filled data points were considered in the regression).

the range of 100–200 μmol quanta m^{-2} s^{-1} and finally stabilizes at a plateau of 2.8 μmol m^{-2} s^{-1}. In order to interrelate the purely photosynthetic O_2 and CO_2 exchange processes, respiratory CO_2 evolution as a function of PAD was subtracted from A_C to obtain the difference A_O–(A_C–R_L). This corrected surplus photosynthetic O_2 evolution rapidly increased from zero to 1.75 μmol m^{-2} s^{-1} at very low PADs and became light-saturated at about 50 μmol m^{-2} s^{-1}. At higher PADs another process appeared to be superimposed, with amplitude of about 0.5 μmol m^{-2} s^{-1} and a light response similar to that of A_O. The example of Fig. 5 was carried out on a plant transferred from NH_4^+ to NO_3^- a week prior to measurement. As a result, the photosynthetic rate and the surplus O_2 evolution processes accelerated significantly in the first newly emerging leaf for all three plants examined. But after a week these rates decreased, approaching the average surplus O_2 evolution rates in NO_3^--grown plants (Fig. 6). In the latter plants it was not possible to

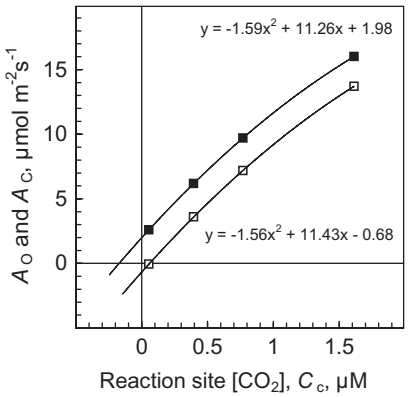

Fig. 4. CO_2 response of O_2 evolution (filled squares) and CO_2 uptake (open squares) rates for the leaf of Fig. 2.

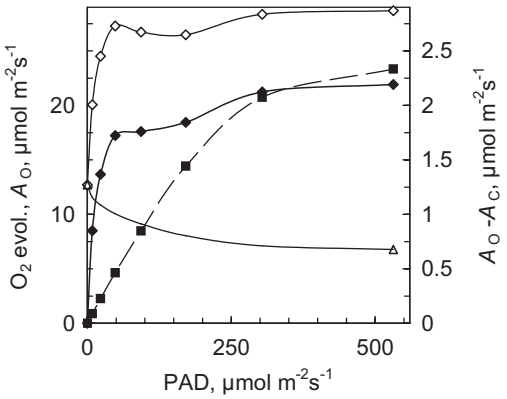

Fig. 5. Light responses of the O_2 evolution rate (filled squares, left ordinate) and of the difference between O_2 and CO_2 exchange rates (A_O–A_C; diamonds, right ordinate). Open diamonds, as measured; filled diamonds, respiration rate subtracted. Respiration rates were measured in the dark and at a PAD of 550 µmol m^{-2} s^{-1} (triangles, right ordinate) as shown in Fig. 4. The latter data points are connected by the light response as modelled by Equation 1 with C=0.47 and α=0.5.

identify the acceptors underlying the two distinct processes supporting surplus O_2 evolution in the light; additional evidence came from investigations with NH_4^+-grown plants.

Assuming the initial (i.e. low PAD) phase of surplus photosynthetic O_2 evolution is related to NO_2^- reduction, it should decrease in NH_4^+-grown leaves, as well as in old leaves that assimilate nitrite slowly. The curves in Figs 6 and 7 confirm this hypothesis. In NH_4^+-grown tobacco leaves (Fig. 6, empty squares), as well as in potato leaves during tuber filling (Fig. 7, empty squares), the highly light-sensitive phase of surplus O_2 evolution is missing, although it was present in potato leaves before flowering. In older leaves, only the component of surplus O_2 evolution with amplitude of 0.6–0.8 µmol m^{-2} s^{-1} and saturating about proportionally with photosynthesis was detectable. This result confirms the presence of two processes of alternative electron transport (surplus O_2 evolution over CO_2 uptake) in leaves, one saturating rapidly at low PADs and the other saturating about proportionally with photosynthesis. The low-light saturating process is referred to below as NO_2^-

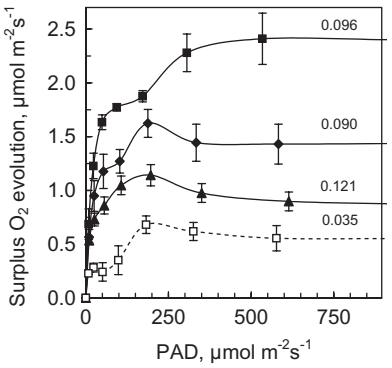

Fig. 6. Surplus photosynthetic O_2 evolution rate as a function of PAD in tobacco leaves grown on NH_4^+ (empty squares), permanently on NO_3^- (filled triangles), and in newly developed leaves 1 week (filled squares) and 2 weeks (filled diamonds) after transfer from NH_4^+ to NO_3^-. Fractional surplus O_2 evolution at light saturation is indicated beside the respective curves. Error bars indicate SD; n=3, except n=6 for filled triangles.

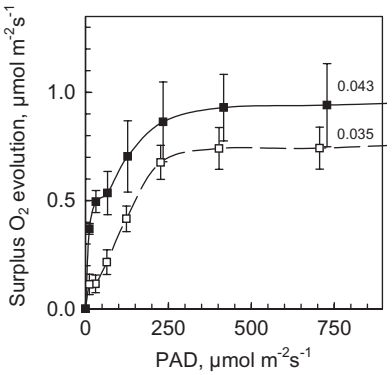

Fig. 7. Light response of surplus O_2 evolution in potato leaves before flowering (filled squares) and during tuber filling (open squares). Fractional surplus O_2 evolution at light saturation is indicated beside the respective curves. Error bars indicate SD, n=4 for filled squares and n=11 for empty squares.

reduction, bearing in mind that about 20% of it may be related to SO_4^{2-} reduction. In NO_2^--reducing leaves the total surplus O_2 evolution accounted for 9–12% of the light-saturated O_2 evolution rate, but in leaves not reducing NO_2^- surplus O_2 evolution was only about 3%.

Quantum yield of electron transport from O_2 evolution versus CO_2 fixation

The relatively fast NO_2^- reduction at low PADs may compete with CO_2 reduction for reducing power and correspondingly decrease the quantum yield of CO_2 uptake. A replot of the data of Fig. 5 shows that O_2 evolution increased linearly with increasing PAD while CO_2 uptake responded sigmoidally (Fig. 8), exhibiting a lower quantum yield for CO_2 uptake at the lowest PADs. The quantum yields of photosynthetic electron transport from O_2 evolution and from CO_2 reduction were calculated and each was plotted against the quantum yield of PSII electron transport

based on Chl fluorescence (Fig. 9). At low PADs the quantum yield from O_2 evolution is directly proportional to the quantum yield of PSII, indicating an extrapolated PSII antenna optical cross-section of 0.52 in the $NH_4^+ \rightarrow NO_3^-$ plant and 0.44 in the NH_4^+-grown plant. In contrast to the quantum yield of electron transport calculated from O_2 evolution, at low PADs the corresponding quantity based on CO_2 uptake is significantly reduced, indicating a rather low PSII optical cross-section for CO_2 reduction. With increasing PAD, as the rate of C reduction becomes faster than the rate of N reduction, the quantum yields of CO_2 uptake and O_2 evolution tend to converge. In NH_4^+-grown plants, low-light suppression of the quantum yield of CO_2 reduction was significantly smaller, though there was a residual effect caused probably by SO_4^{2-} and disulfide reduction.

The light response curve of CO_2 uptake was also measured at the normal atmospheric O_2 level of 210 mmol mol^{-1} (measurement of O_2 evolution was not possible with the necessary precision at this high background O_2 concentration). The electron transport rate supporting CO_2 reduction was calculated considering both net photosynthesis and photorespiration, as determined by CO_2 and O_2 concentrations at the Rubisco active sites, Rubisco CO_2/O_2 specificity (Laisk and Oja, 1998; Laisk *et al.*, 2002) and, arbitrarily, assuming a light response of 'dark' respiration identical to the anaerobic condition. At this high O_2 level the plot showed considerably less NO_2^- reduction competing with CO_2 reduction than under the anaerobic condition.

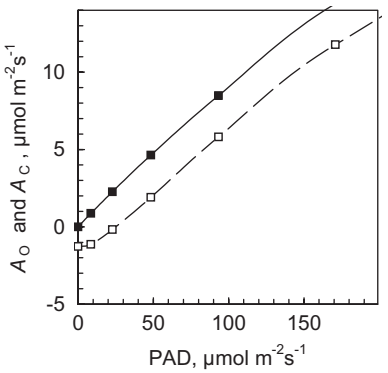

Fig. 8. Light response curves of O_2 evolution (filled symbols) and CO_2 uptake (empty symbols) for the tobacco plant of Fig. 5, 1 week after $NH_4^+ \rightarrow NO_3^-$ transfer.

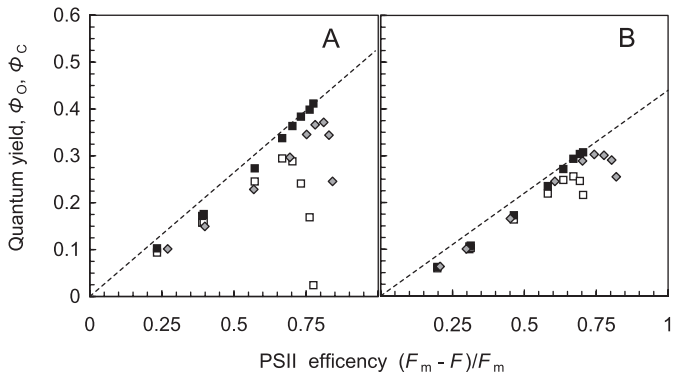

Fig. 9. Quantum yield of photosynthetic electron transport calculated as $\Phi_O = A_O/PAD$ (filled squares) and $\Phi_C = 4A_C/PAD$ (empty squares) and plotted against the quantum yield of PSII calculated as $\Phi_{II} = (F_m - F)/F_m$. (A) The tobacco plant of Fig. 5, 1 week after $NH_4^+ \rightarrow NO_3^-$ transfer. (B) An NH_4^+-grown plant. For comparison, the quantum yield of photosynthetic electron transport was calculated (see text) from measurements of net H_2O and CO_2 exchange which consider photorespiration in the presence of 21% O_2 and 360 ppm CO_2 (grey diamonds).

Surplus O_2 evolution in C_4 plants

Similar experiments were carried with the NADP-ME type C_4 plant *Sorghum bicolor* and the NAD-ME type C_4 plant *Amaranthus edulis* both grown on NH_4NO_3. Both C_4 plants exhibited surplus O_2 evolution at low PADs as well as the component proportional to photosynthesis at high PADs (Fig. 10; Table 1). The low-PAD component was faster in amaranth compared with sorghum (only the older leaves of which could be fitted to the leaf chamber), but the second component was larger in sorghum. There was a narrow range of PADs (100–200 μmol m^{-2} s^{-1}) where surplus O_2 evolution exhibited a minimum.

Does electron flow to O_2 occur?

The experiments described above confirm the feasibility of balancing ATP synthesis to reductant utilization by directing a portion of linear electron flow to NO_2^- and OA. Although anaerobic conditions precluded significant photoreduction of O_2 it is relevant to consider whether Mehler-type processes could contribute to ATP-balancing by coupling electron transport to H^+ translocation when O_2 is present. The *Arabidopsis aba 1-6* mutant possesses constitutively high levels of zeaxanthin ensuring a rapid, sensitive, and reversible response to changes in thylakoid lumen pH. In an earlier study, Laisk *et al.* (2010) showed that omission of CO_2 caused a dramatic shift in the light response of the H^+-dependent phase of NPQ (qE) to lower PADs. Using a similar approach, Fig. 11 compares *qE* to the linear

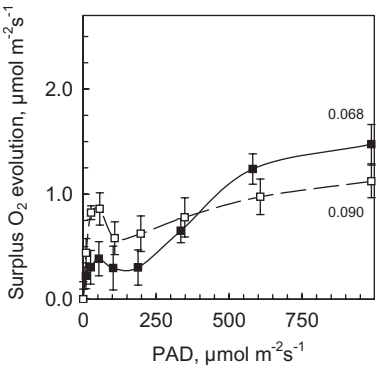

Fig. 10. Light responses of surplus O_2 evolution in sorghum (filled symbols) and amaranth (empty symbols) grown on NH_4NO_3. Fractional surplus O_2 evolution at light saturation is indicated beside each curve. Error bars indicate SD, n=4.

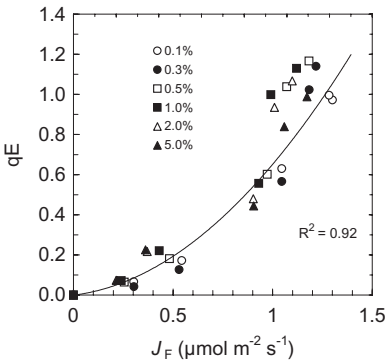

Fig. 11. Relationship between H^+-dependent qE formation and rate of linear photosynthetic electron transport based on Chl fluorescence (J_F) with increasing O_2 level. Leaves of *Arabidopsis* mutant *aba 1-6* were first exposed to increasing PADs ranging from zero to 9.0 μmol quanta m^{-2} s^{-1} at 23 °C in CO_2-free 0.1% O_2 (balance N_2). At each PAD, NPQ_{PAD} was measured as F_{md}/F_m–1 where F_{md} is the 'predawn' maximum fluorescence yield. Light response curves were similarly recorded for all O_2 levels shown. The qE phase was isolated as NPQ_{PAD} minus NPQ_0 (measured prior in darkness) to exclude the effects of progressive accumulation of H^+-independent photoinhibitory quenching. Error bars are omitted for clarity and n=3. The line is a parabolic fit to all data. For additional details see Laisk *et al.* (2010).

electron transport rate based on Chl fluorescence (J_F) over a 50-fold range of gas phase O_2 levels when CO_2 was absent. The results offer no indication of an O_2-dependent enhancement of *qE* formation over this range.

Discussion

As noted in the Introduction, most simultaneous measurements of O_2 evolution and CO_2 uptake have been carried out on the background of the atmospheric O_2 concentration. This extremely difficult technical task was solved at a resolution of ±2 ppm on a background of 210 000 ppm O_2 (Bloom *et al.*, 1989). In wild-type barley plants receiving ammonium as the sole nitrogen source or in nitrate reductase-deficient mutants, photosynthetic and respiratory fluxes of oxygen equalled those of carbon dioxide. By contrast, in wild-type plants growing on nitrate in high light, O_2 evolution exceeded carbon dioxide consumption by 26% and, in the dark, carbon dioxide evolution exceeded oxygen consumption by 25%. Similar measurements with shifts from ammonium to nitrate nutrition (Bloom *et al.*, 1992) indicated that, under NH_4^+ nutrition, 14% of root carbon catabolism is coupled to NH_4^+ assimilation. Under NO_3^- nutrition, 5% of root carbon catabolism is coupled to NO_3^- absorption, 15% to NO_3^- assimilation, and 3% to NH_4^+ assimilation. The additional energy requirements of NO_3^- assimilation diminished root mitochondrial electron transport. The most conclusive integral measurements of this type showed that less than 45% of nitrate was reduced in roots of white lupin and soybean (Cen *et al.*, 2001; Cen and Layzell, 2003). The photosynthetic O_2/CO_2 ratio was 1.026 while the respiratory CO_2/O_2 ratio was 1.12, indicating that relatively more reducing power is diverted to alternative reductions during respiration compared with photosynthesis, but absolute rates of photosynthesis are much greater than those of respiration.

Photorespiration has been viewed as an unfavourable consequence of plant evolution under an atmosphere that contained much higher levels of carbon dioxide than it does today. The exposure of *Arabidopsis* and wheat shoots to conditions that inhibited photorespiration strongly inhibited nitrate assimilation (Rachmilevitch *et al.*, 2004). Short-term exposures to elevated CO_2 concentrations diverted photosynthetic reductant from NO_3^- or NO_2^- reduction to CO_2 fixation in *Triticum aestivum* (Bloom *et al.*, 2002). Accordingly, when wheat plants received NO_3^- rather than NH_4^+ as a nitrogen source, CO_2 enhancement of shoot growth halved and CO_2 inhibition of shoot protein synthesis doubled. These net gas exchange measurements were complemented by chlorophyll fluorescence measurements, from which the PSII electron transport J_{II} was calculated (Genty *et al.*, 1989) and the gross O_2 evolution was calculated as $J_{II}/4$ (Cousins and Bloom, 2004). Under the ambient CO_2 concentration the net O_2 exchange increased in wheat plants receiving NO_3^- instead of NH_4^+, but gross O_2 evolution from the photosynthetic apparatus was insensitive to nitrogen source. Therefore, O_2 consumption within wheat photosynthetic tissue decreased during NO_3^- assimilation. The data were interpreted to show that, in wheat, a C_3 plant, mitochondrial respiration is decreased during NO_3^- assimilation. However, in maize, a C_4 plant, NO_3^- assimilation appeared to stimulate mitochondrial respiration.

These results indicated that a substantial portion of photosynthetic electron transport or respiratory organic acid degradation generates reductant for nitrate assimilation rather than for carbon fixation or mitochondrial electron transport. Nitrate assimilation in both dicotyledonous and monocotyledonous species depends on photorespiration. This role for photorespiration explains several responses of plants to rising carbon dioxide concentrations, including the inability of many plants to sustain rapid growth under elevated levels of carbon dioxide; and raises concerns about genetic manipulations to diminish photorespiration in crops.

In this work, the focus was on the branching of photosynthetically generated reductant between carbon and nitrite reduction processes in leaf chloroplasts. Respiratory O_2 uptake was effectively abolished under anaerobiosis, but CO_2 evolution from dark respiration was not significantly suppressed during the measurements either in NO_3^-- or NH_4^+-grown leaves. For example, when O_2 was rapidly removed in the dark, no transients in CO_2 evolution occurred, indicating facile adjustment between aerobic to the anaerobic metabolism (data not shown). Thus, electron flow arising from the respiratory carbohydrate and organic acid catabolism was immediately and smoothly diverted from O_2 reduction to alternative reductant utilization processes, perhaps NO_3^- reduction and lipid synthesis. Under anaerobiosis, the NADH level was probably elevated, as

occurs in the CMS mutant of *Nicotiana sylvestris* lacking Complex I of the mitochondrial electron transport chain (Dutilleul *et al.*, 2005). Therefore, if NO_3^- mobilization is controlled by the NADH/NAD ratio then rates of NO_2^- reduction during our anaerobic exposures could exceed those occurring under normal atmospheric conditions (neglecting the fast cycling of ammonia during photorespiratory metabolism; Rachmilevitch *et al.*, 2004). The enhanced NO_2^- reduction at the low O_2 concentration (Robinson, 1990) was indeed indicated by the quantum yield data where CO_2 reduction was more efficiently outcompeted by NO_2^- reduction compared with the air level of O_2 (Fig. 9). Thus, the reported absolute rates of NO_2^- reduction during anaerobiosis exceed those during growth in normal air. Nevertheless, this in no way diminishes the reliability of our mechanistic conclusions.

The major focus of this work is the interaction of C and N assimilation processes during photosynthesis. We elaborated on our previous approaches (Laisk *et al.*, 2006, 2007) by considering light-dependent suppression of respiratory CO_2 evolution. It is worthwhile to note that suppression of anaerobic respiratory CO_2 evolution in the light indicates that the interaction between photosynthesis and respiration occurs via carbon metabolism and not at the level of the mitochondrial electron transport chain. Accurate consideration of respiratory CO_2 evolution is important for the quantification of photosynthetic O_2–CO_2 flux differences that are comparable in magnitude. The results showed a dual phase light response for surplus photosynthetic O_2 evolution in NO_3^--grown plants. Surplus O_2 evolution increased sharply with increasing PAD to 1.0–1.5 μmol O_2 m^{-2} s^{-1} and saturated at a PAD of about 50 μmol m^{-2} s^{-1}. At higher PADs another process with amplitude of 0.5–1 μmol O_2 m^{-2} s^{-1} approached light saturation approximately in parallel with photosynthesis. By contrast, in NH_4^+-grown tobacco, as well as in potato leaves during tuber filling, the low-light component of surplus O_2 evolution was only 0.1–0.2 μmol m^{-2} s^{-1}. These dramatic effects of N source during growth lead us to ascribe the initial phase of surplus O_2 evolution to photosynthetic NO_2^- reduction. This is also supported by the fact that in older leaves excess O_2 evolution was very slow (Table 1; sorghum, potato) consistent with preferential localization of N assimilation for protein accumulation in young, expanding leaves. The high-light component is suggested to be associated with oxaloacetate reduction (Mehler-type O_2 reduction and photorespiration were absent under the anaerobic conditions employed).

According to these results, maximum photosynthetic NO_2^- reduction rates are 0.67–1.0 μmol m^{-2} s^{-1}, equivalent to about 2 μmol NO_2^- mg^{-1} Chl h^{-1}. This rate is significantly lower than the value of 4–8 μmol NO_2^- mg^{-1} Chl h^{-1} recorded in isolated spinach chloroplasts and mesophyll cells under saturating NO_2^- (Robinson, 1988). This shows that the enzymic capacity of the NO_2^- reduction pathway exceeds the maximum rate observed in leaves, indicating probable limitation by availability of NO_2^- or amino acceptor OG.

An important question concerns the competition between CO_2 and NO_2^- reduction pathways for photosynthetic reductant (Baysdorfer and Robinson, 1985; Robinson, 1986; 1988). If free Fd^- in the stroma is the substrate for FNR and NiR then competition between the two pathways is inevitable (Meyer and Stöhr, 2002). The two reduction pathways may function independently only if Fd^- is compartmented separately for FNR and NiR, for example, if NiR and GOGAT systems are connected to a small fraction, while FNR is connected to the majority, of PSI centres. However, if this hypothesis was true then both rates would increase proportionally with light intensity, but the quantum yield of NO_2^- reduction would be much lower than that of CO_2 reduction. Our results, and actually those of Robinson (1988), do not support this hypothesis, and instead show that at low PADs NO_2^- reduction increases with a quantum yield comparable to that of CO_2 reduction (Table 1). Furthermore, NO_2^- reduction saturates at a low PAD of about 50 μmol quanta m^{-2} s^{-1} while CO_2 reduction continues to increase with light intensity. Our results (Fig. 9) indicate that, at PADs <50 μmol quanta m^{-2} s^{-1}, the quantum yield of CO_2 fixation is still lower than that of O_2 evolution when NO_2^- assimilation is suppressed (NH_4^+-grown plants) but these differences are much smaller than observed in NO_3^--grown plants. For the latter plants at a very low PAD of 10 μmol quanta m^{-2} s^{-1}, the quantum yield of CO_2 reduction was substantially lower than O_2 evolution, indicating that FNR was strongly out-competed by NiR (and possibly by other alternative electron acceptors, e.g. SO_4^{-2} and disulphide groups). At 30 μmol quanta m^{-2} s^{-1} the quantum yield of CO_2 fixation was about one-half of the maximum, indicating about equal competitive affinities of NiR and FNR for Fd^-. Robinson (1988) drew the opposite conclusion from similar experiments, because he did not study the two rates in sufficient detail at low PADs. At higher PADs where NO_2^- reduction is light-saturated, and thus constant, it can no longer compete with CO_2 reduction. The O_2/CO_2 flux measurements were similarly misinterpreted over a range of high PADs, where excess O_2 evolution increased minimally with PAD (Laisk *et al.*, 2007). The results of this work thus allow us to conclude that NiR and FNR both compete for one and the same pool of Fd^- with rather similar affinities (or NiR even in excess). The NiR pathway saturates at a low light intensity and a low rate, while the FNR pathway accelerates with increasing light to a rate about 10–20 times faster than the NiR rate.

This work was initiated under the proposition that NO_2^- reduction corrects imbalances in ATP/NADPH stoichiometries during photosynthesis (Noctor and Foyer, 1998; Laisk *et al.*, 2009). Our tobacco plants did grow slower on NH_4^+ than on NO_3^-. Such an inhibitory effect of ammonia has been attributed to an ill-defined 'toxicity'. High ammonium is known to uncouple chloroplast and mitochondrial electron transport and thus disrupt pH gradients. However, no lingering signs of uncoupling were seen in our NH_4^+-grown plants. The fact that the apparent toxicity of NH_4^+ is different among species and growth conditions, and depends on the rate of the nutrient supply (Roosta *et al.*,

2009), suggests that it is actually caused by an imbalance involving a combination of ammonia and other metabolic conditions. For example, it is well known that NH_4^+ and NO_3^- together constitute an optimal plant N source. Our NH_4^+-grown leaves grew small, thick, and full of starch, an indication of normal photosynthesis, but possible limitation in protein synthesis due to the absence of NO_2^--supported extra ATP production. However, in these plants the high-light component of surplus O_2 evolution, which is ascribed to OA reduction, exhibited rates of 0.5–1 μmol m^{-2} s^{-1}, or about 3.5% of the maximum photosynthetic rate (Fig. 6; Table 1). Such a rate of OA reduction was just enough to generate the extra ATP needed for the accumulation of starch. It is therefore suggested that, in the NH_4^+-grown plants, ammonia is available, but protein synthesis is limited by an ATP deficit caused by a limitation in alternative electron transport. At higher PADs some extra ATP is available due to OA reduction, but this ATP is preferentially employed for starch rather than protein synthesis. Surprisingly, when present, O_2 failed to enhance H^+ translocation as indicated by qE formation (Fig. 11) suggesting that production of extra ATP is obligatorily linked to NO_2^- and OA reduction.

In NO_3^--grown plants, protein synthesis was adequately supported by ATP synthesized at the expense of excess electron transport for NO_2^- reduction at low PADs. For example, at a PAD of 50 μmol m^{-2} s^{-1} surplus O_2 evolution comprised 20–30% of the total electron flow (Table 1). In the $NH_4^+ \rightarrow NO_3^-$ transfer experiment ammonium ion initially inhibited growth, but 'toxicity' was relieved once the endogenous NH_4^+ pool was combined with exogenous NO_3^-. The burst of leaf growth suggests that rapid protein synthesis became possible only after NO_2^- reduction began. This supports the notion that an optimum in amino acid and ATP availability for protein synthesis is achieved under combined nutrition with NO_3^- and NH_4^+.

Surplus O_2 evolution was quite similar in C_3 and C_4 plants. Photoreduction of O_2 was largely absent under the low O_2 concentration in our experiments, nevertheless, the photosynthetic rate was high. This shows that the relatively high rate of O_2 reduction reported in C_4 plants under atmospheric O_2 concentration (Siebke *et al.*, 2003) is not essential for extra ATP production in the bundle sheath cells.

In conclusion, the results of this work support the contention that NO_2^- and CO_2 assimilation processes interact at the level of photosynthetic electron transport and a control point for their mutual regulation is on the reducing side of PSI. Nitrite reductase successfully competes with ferredoxin-NADP reductase for reduced ferredoxin at low light intensities, but NO_2^- reduction becomes saturated at low light intensities at a low rate so that it can no longer compete with FNR at high light intensities. NO_2^- reduction supports ATP synthesis for alternative uses, specifically for protein and starch synthesis in chloroplasts. In the absence of NO_2^- reduction starch may still be synthesized using extra ATP produced during OA reduction. No essential nor optional role for Mehler-type O_2 photoreduction in ATP-balancing is indicated.

Acknowledgements

This work was supported by targeted financing theme SF0180045s08 from the Estonian Ministry of Education and Science, grants 8283 and 8344 from the Estonian Science Foundation, and Hatch funding from the US Department of Agriculture. Technical assistance by E. Talts is highly appreciated.

References

Anderson JW, Done J. 1978. Light-dependent assimilation of nitrite by isolated pea chloroplasts. *Plant Physiology* **61,** 692–697.

Badger MR, von Caemmerer S, Ruuska S, Nakano H. 2000. Electron flow to oxygen in higher plants and algae: rate and control of direct photoreduction (Mehler reaction) and Rubisco oxygenase. *Philosophical Transactions of the Royal Society of London, Series B* **355,** 1433–1446.

Baysdorfer C, Robinson JM. 1985. Metabolic interactions between spinach leaf nitrite reductase and ferrodoxin-NADP reductase. *Plant Physiology* **77,** 318–320.

Björkman O, Gauhl E. 1970. Use of zirconium oxide ceramic cell for measurements of photosynthetic oxygen evolution intact leaves. *Photosynthetica* **4,** 123–128.

Bloom AJ, Caldwell RM, Finazzo J, Warner RL, Weissbart J. 1989. Oxygen and carbon dioxide fluxes from barley shoots depend on nitrate assimilation. *Plant Physiology* **91,** 352–356.

Bloom AJ, Sukrapanna SS, Warner RL. 1992. Root respiration associated with ammonium and nitrate absorption and assimilation by barley. *Plant Physiology* **99,** 1294–1301.

Bloom AJ, Smart DR, Nguyen DT, Searles PS. 2002. Nitrogen assimilation and growth of wheat under elevated carbon dioxide. *Proceedings of the National Academy of Sciences, USA* **99,** 1730–1735.

Brunswick P, Cresswell CF. 1988*a*. Nitrite uptake into intact pea chloroplasts. I. Kinetics and relationship with nitrate assimilation. *Plant Physiology* **86,** 378–383.

Brunswick P, Cresswell CF. 1988*b*. Nitrite uptake into intact pea chloroplasts. II. Influence of electron transport regulators, uncouplers, ATPase and anion uptake inhibitors and protein binding reagents. *Plant Physiology* **86,** 384–389.

Cen Y-P, Turpin DH, Layzell DB. 2001. Whole-plant gas exchange and reductive biosynthesis in white lupin. *Plant Physiology* **126,** 1555–1565.

Cen Y-P, Layzell DB. 2003. *In vivo* gas exchange measurement of the site and dynamics of nitrate reduction in soybean. *Plant Physiology* **131,** 1147–1156.

Cousins AB, Bloom AJ. 2004. Oxygen consumption during leaf nitrate assimilation in a C3 and C4 plant: the role of mitochondrial respiration. *Plant, Cell and Environment* **27,** 1537–1545.

Dutilleul C, Lelarge C, Prioul J-L, De Paepe R, Foyer CH. 2005. Mitochondria-driven changes in leaf NAD status exert a crucial influence on the control of nitrate assimilation and the integration of carbon and nitrogen metabolism. *Plant Physiology* **139,** 64–78.

Eichelmann H, Talts E, Oja V, Padu E, Laisk A. 2009. Rubisco *in planta* k_{cat} is regulated in balance with photosynthetic electron transport. *Journal of Experimental Botany* **60,** 4077–4088.

Foyer CH, Noctor G. 2002. Photosynthetic nitrogen assimilation: inter-pathway control and signaling. In: Foyer CH, Noctor G, eds. *Photosynthetic nitrogen assimilation and associated carbon and respiratory metabolism*. Dordrecht/Boston/London: Kluwer Academic Publishers, 1–22.

Genty B, Briantais JM, Baker NR. 1989. The relationship between quantum yield of photosynthetic electron transport and quenching of chlorophyll fluorescence *Biochimica et Biophysica Acta* **990,** 87–92.

Hirasawa M, Nakayama M, Hase T, Knaff DB. 2004. Oxidation–reduction properties of maize ferredoxin:sulfite oxidoreductase. *Biochimica et Biophysica Acta* **1608,** 140–148.

Kirschbaum MUF, Pearcy RW. 1988. Concurrent measurements of oxygen- and carbon-dioxide exchange during lightflecks in *Alocasia macrorrhiza* (L.) G.Don. *Planta* **174,** 527–533.

Kopriva S. 2006. Regulation of sulfate assimilation in *Arabidopsis* and beyond. *Annals of Botany* **97,** 479–495.

Laisk A, Eichelmann H, Oja V. 2009. Leaf C3 photosynthesis *in silico*: integrated carbon/nitrogen metabolism. In: Laisk A, Nedbal L, Govindjee, eds. *Photosynthesis in silico: understanding complexity from molecules to ecosystems*. The Netherlands: Springer Science+Business Media BV, 295–322.

Laisk A, Eichelmann H, Oja V, Rasulov B, Rämma H. 2006. Photosystem II cycle and alternative electron flow in leaves. *Plant and Cell Physiology* **47,** 972–983.

Laisk A, Eichelmann H, Oja V, Talts E, Scheibe R. 2007. Rates and roles of cyclic and alternative electron flow in potato leaves. *Plant and Cell Physiology* **48,** 1575–1588.

Laisk Oja V. 1998. *Dynamic gas exchange of leaf photosynthesis. Measurement and interpretation*. Collingwood: CSIRO Publishing.

Laisk A, Oja V, Eichelmann H. 2007. Kinetics of leaf oxygen uptake represent *in planta* activities of respiratory electron transport and terminal oxidases. *Physiologia Plantarum* **131,** 1–9.

Laisk A, Oja V, Eichelmann H. 2008. Alternative and cyclic electron flow: rate and role in potato leaves. In: Allen JF, Gantt E, Golbeck JH, Osmond B, eds. *Photosynthesis. Energy from the sun.* 14th International Congress on Photosynthesis. Springer, 913–916.

Laisk A, Oja V, Rasulov B, Rämma H, Eichelmann H, Kasparova I, Pettai H, Padu E, Vapaavuori E. 2002. A computer-operated routine of gas exchange and optical measurements to diagnose photosynthetic apparatus in leaves. *Plant, Cell and Environment* **25,** 923–943.

Laisk A, Talts E, Oja V, Eichelmann H, Peterson R. 2010. Fast cyclic electron transport around photosystem I in leaves under far-red light: a proton-uncoupled pathway? *Photosynthesis Research* **103,** 79–95.

Meyer C, Stöhr C. 2002. Soluble and plasma membrane-bound enzymes involved in nitrate and nitrite metabolism. In: Foyer CH, Noctor G, eds. *Photosynthetic nitrogen assimilation and associated carbon and respiratory metabolism*. Dordrecht/Boston/London: Kluwer Academic Publishers, 49–62.

Noctor G, Foyer CH. 1998. A re-evaluation of the ATP: NADPH budget during C_3 photosynthesis: a contribution from nitrate assimilation and its associated respiratory activity? *Journal of Experimental Botany* **49,** 1895–1908.

Oja V, Eichelmann H, Anijalg A, Rämma H, Laisk A. 2010. Equilibrium or disequilibrium? A dual-wavelength investigation of photosystem I donors. *Photosynthesis Research* **103,** 153–166.

Oja V, Eichelmann H, Laisk A. 2007. Calibration of simultaneous measurements of photosynthetic carbon dioxide uptake and oxygen evolution in leaves. *Plant and Cell Physiology* **48,** 198–203.

Oja V, Eichelmann H, Peterson RB, Rasulov B, Laisk A. 2003. Decyphering the 820 nm signal: redox state of donor side and quantum yield of photosystem I in leaves. *Photosynthesis Research* **78,** 1–15.

Rachmilevitch S, Cousins AB, Bloom AJ. 2004. Nitrate assimilation depends on photorespiration. *Proceedings of the National Academy of Sciences, USA* **101,** 11506–11510.

Robinson JM. 1986. Carbon dioxide and nitrite photoassimilatory processes do not intercompete for reducing equivalents in spinach and soybean leaf chloroplasts. *Plant Physiology* **80,** 676–684.

Robinson JM. 1988. Spinach leaf chloroplast CO_2 and NO_2^- photoassimilations do not compete for photogenerated reductant. *Plant Physiology* **88,** 1373–1380.

Robinson JM. 1990. Nitrite photoreduction *in vivo* is inhibited by oxygen. *Plant Physiology* **92,** 862–865.

Roosta HR, Sajjadinia A, Rahimi A, Schjoerring JK. 2009. Responses of cucumber plant to NH_4^+ and NO_3^- nutrition: the relative addition rate techniques vs. cultivation at constant nitrogen concentration. *Scientia Horticulturae* **121,** 397–403.

Ruuska SA, Badger MR, Andrews TJ, von Caemmerer S. 2000. Photosynthetic electron sinks in in transgenic tobacco with reduced amounts of Rubisco: little evidence for significant Mehler reaction. *Journal of Experimental Botany* **51,** 357–368.

Shingles R, Roh MH, McCarty RE. 1996. Nitrite transport in chloroplast inner envelope vesicles. I. Direct measurement of proton-linked transport. *Plant Physiology* **112,** 1375–1381.

Siebke K, Ghannoum O, Conroy JP, Badger MR, von Caemmerer S. 2003. Photosynthetic oxygen exchange in C4 grasses: the role of oxygen as electron acceptor. *Plant, Cell and Environment* **26,** 1963–1972.

Swader JA, Stocking CR. 1971. Nitrate and nitrite reduction by *Wolffia arrhiza*. *Plant Physiology* **47,** 189–191.

Warburg O. 1948. Assimilatory quotient and photochemical yield. *American Journal of Botany* **35,** 194–204.